Tensile Behaviour of S690QL and S960QL under High Strain Rate

A. A. Alabi[1,2,*], P. L. Moore[3], L. C. Wrobel[1], J. C. Campbell[1,2], W. He[4]
[1]Department of Mechanical and Aerospace Engineering, Brunel University London, Uxbridge, UK
[2]National Structural Integrity Research Centre (NSIRC), Granta Park, Great Abington, Cambridge, UK
[3]TWI Ltd, Granta Park, Great Abington, Cambridge, UK
[4]Lloyds Register Global Technology Centre, Southampton, UK

Abstract
Despite offering significant strength-to-weight advantages, high-strength structural steels, such as S690QL and S960QL, are used only in limited offshore applications. This is due to the lack of material characterisation in regard to their tensile behaviour, with little data available on loading rates other than those typically experienced offshore. The concern is that high strength structural steels with high yield-to-tensile ratio >0.90 are obtained at the expense of ductility and strain-hardening capacity. In this paper the tensile properties from two high strength structural steels were studied and characterised over a range of strain rates and, the results are compared against the performance of mild steel. High strength structural steels with yield-to-tensile ratios in excess of 0.90 were significantly less sensitive to the effect of strain rate than mild steel with yield-to-tensile < 0.85 at ambient temperature. The yield stress of S690QL and S960QL moderately increase to about 9% and 6% respectively from quasi-static to 100 s^{-1} strain rate, which is within typical strain rates encountered in primary offshore structural applications.

---

* Corresponding author at: National Structural Integrity Research Centre (NSIRC), Granta Park, Great Abington, Cambridge, CB21 6AL, United Kingdom
E-mail address: aderinkola.alabi@brunel.ac.uk (A. A. Alabi)

1. Introduction

The main driving force in the development and usage of high strength structural steel (HSSS) in offshore applications is the need to reduce weight and cost over structures manufactured from conventional low strength structural grades. Modern production routes for HSSS grades deliver high yield strengths, but with much higher yield-to-tensile (Y/T) ratios than in lower strength structural steel grades (LSSS). This high Y/T ratio results in existing standards lacking clear guidance for the application and performance of modern high strength steel. Eurocode 3 (Design of Steel Structures), EN 1993: Part 1-12 [1] recommends a limit of 0.95 Y/T ratio, whereas the UK National Annex of the same standard proposed a value of 0.91 [2] due to lack of confidence regarding the performance of HSSS with high Y/T ratio in the standards. Most design codes and standards relate the design formulae to mild strength steel with low Y/T ratio < 0.85 and yield strength < 500 MPa for offshore design requirement [3,4], limiting the overall usage of HSSS in offshore steel structural applications. This is because the performance of LSSS is well established, and also provides an enhanced safety margin (a proportion of the yield strength against the ultimate tensile strength) with which the same confidence with HSSS is not known. A concern is that higher yield strength with Y/T > 0.9 may be obtained at the expense of ductility and strain-hardening capacity, compromising the post-yield strength upon which design criteria depend when compared to LSSS with Y/T < 0.8 [4,5]. As confidence in the characterisation and performance of steels with Y/T ratios in excess of 0.90 is established, they will become more accepted into design codes and standards. HSSS would then be exploited for its strength, but not rely on its ability to deform or locally yield under extreme loading because HSSS steel structures offer significant benefits which include a greater reduction in capital cost (economy), improved mechanical properties (safety), and development of special aesthetic and elegant designs with reduced structural section (architecture).

Hence, the motivation of this research is to reverse the under-utilization of HSSS for various applications through developing a better understanding and characterisation of the behaviour of HSSS grades with high Y/T ratios > 0.90 under different loading conditions and determine their sensitivity to in-service loading rates, such as those given in **Table 1** where there is a chance of reduced ductility at dynamic loading rates. For example, Eurocode 3 (Design of Steel Structures) now has an extension up to S700 (S690QL equivalent) in EN 1993: Part 1-12 [1] due to the need to reduce weight with increased strength capacity, coupled with the cost effectiveness. This standard allows S700 utilization but with a limitation of Y/T ratio between 0.91 and 0.95 for bridges, buildings and other steel structures [1,2].

Compared with other published data and experimental results from conventional low strength carbon steel tensile tests, modern high strength steel possesses a different stress-strain characteristic, reduced elongation and low strain-hardening capacity and, generally, has high Y/T ratio [6,7]. In addition, very little information is available on the performance of HSSS (specifically, with Y/T in excess of 0.90) subjected to high loading rate scenarios. It is noteworthy that the effect of high loading rates is generally known to affect the strength and fracture performance of steels [8-17]. Invariably, the effect of loading rates on the tensile properties or strength of a steel is predicted to be specifically dependent on a particular steel grade [8,9] with the sensitivity depending on the strength level itself. The degree of sensitivity, however, on the low strength carbon steels is high compared to quenched and tempered and High Strength Low Alloyed (HSLA) steels, which are relatively unaffected [10]. Typical examples of engineering loading rates expressed in terms of

strain rate are given in **Table 1**. These values are taken from the information given by **[11-13]**, and should be used as estimates only since the exact values will depend largely on loading configuration, local geometry, and flaw dimensions **[12]**. Whilst the fracture mechanical loading rate is mostly expressed in terms of stress intensity factor loading rate for linear elastic conditions, the loading rates in structural engineering are usually considered in terms of strain rates **[8].** Therefore, for the purpose of this paper, loading rates in terms of strain rate have been considered.

The effect of loading rates on the tensile properties of typical high strength structural steels, namely S690QL and S960QL, produced via quenched and tempered (QT) processing routes has been studied. The degree of strain rate sensitivity is compared with the performance of low strength conventional structural steel, S235 at ambient temperature. It should be noted that the main purpose of this work is to study the tensile behaviour of HSSS with high Y/T ratio > 0.90 and not LSSS grades with low Y/T ratio < 0.80. The conventional structural steel S235 was used as an example of low Y/T ratio grade that has been previously well characterised for dynamic behaviour, although not used significantly in offshore applications. The findings and data generated would help to better understand the structural performance of HSSS with high Y/T ratio and, thus, reduce the misconceptions of its performance in design guidelines and in-service.

Table 1: Typical strain rates in some engineering components. Data from **[11-13]**

Application	Strain Rate $(\dot{\varepsilon})$ s^{-1}
Storage Tanks, Buried Pipelines, Pressure Vessels	10^{-6} to 10^{-4}
Self-Weight, Wind and Wave Loading,	10^{-4} to 10^{-2}
Bridges, Cranes, Earthmoving	10^{-2} to 0.1
Earthquake loading, Marine collisions	0.1 to 10
Land transport, Aircraft undercarriage	10 to 10^3
Explosion, Ballistics	10^4 to 10^{6+}

2. Review of strain rate effects on the tensile properties of structural steels

The major strain rate effect on the tensile properties of steel is the amplification of the yield and tensile strengths, considered as a positive strain rate dependence **[12]**. On the other hand, the increment could result in a shift in the Ductile-to-Brittle Transition Curve (DBTC) leading to a reduced fracture toughness value at the lower shelf as a result of material strengthening during an increase in strain rate (negative strain rate dependence) **[8,12]**. The behaviour of carbon steels at high strain rates shows that both the upper and lower yield stresses and strains increase with increasing strain rates **[9]**. However, the ultimate stress and strain are less sensitive at high strain rates, whereas the strain at initiation of strain hardening is the most sensitive parameter to the effect of strain rate **[9]**. Another important aspect of strain rate effect on the tensile properties of steel is the temperature dependence. The effect of high strain rate and consequently, the dynamic amplification on yield strength is temperature dependent, being increased at lower temperature **[8-10,12-18]**. In general terms, the yield strength of a particular material under dynamic loading (high strain rate) is strain rate and temperature dependent, linearly related to the logarithm of the strain rate and inversely proportional to the absolute temperature as expressed in Eq. (1) **[10]**.

The dynamic yield strength was observed to be equal to the static yield strength plus a factor which causes an increase (or decrease) in the tensile properties called the

dynamic over stress **[10]**. The dynamic over stress is temperature dependent and implies that at low temperature, the dynamic over stress increases owing to the strain rate effects, but decreases with thermal softening at high temperature.

$$\sigma_{yd} = \sigma_y (T, \dot{\varepsilon}) \approx \frac{\ln(\dot{\varepsilon})}{T} \qquad (1)$$

This is explained by the mechanism of thermal activation of dislocations over short-range barriers **[13,18]**. Since a dislocation is obstructed in its movement by the interstitial atoms (such as, carbon, nitrogen, boron or hydrogen) or grain boundaries in steel, it means that a higher force is required to overcome this obstruction. A stress (flow stress) is required to sustain plastic deformation by moving dislocations via both short and long range barriers, with its magnitude depending on the temperature **[13]**. Over short-range barriers, there exists an initial stress large enough to enable the dislocations to move past these barriers without the aid of thermal fluctuations associated with yield stress at absolute zero temperature. It follows that at stresses greater than the initial stress, the barriers are ineffective and the strain rate is then controlled by a different mechanism (dissipative mechanism), such as the interaction of dislocations with electrical and thermal waves in the crystal lattice **[18]**. If deformation is thermally activated **Figure 1**, the effective stress σ^* is strain rate and temperature dependent due to short-range barriers that can be cut or passed by thermal activation, which is characterised by activation enthalpy, Eq. (2) **[13]**.
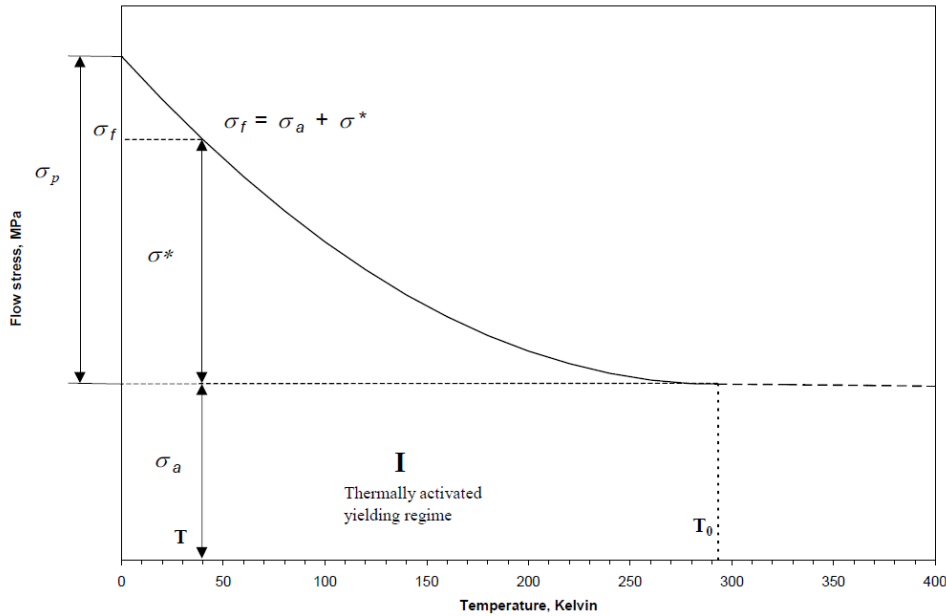

Figure 1: Flow stress partitions of an effective stress and internal stress with temperature of interest less 300 K [**13**]. Courtesy of TWI Ltd.

The value of flow stress can therefore be characterised varying from a maximum value $(\sigma_p+\sigma_a)$ to an athermal internal stress value σ_a at temperature T_0, Figure 1 **[13]**. At athermal (long range barriers) condition, the increased amplitude of atomic thermal vibrations produces an effective vibration of the dislocation line, and this permits it to cut through barriers that could not be bypassed by the stress alone and,

thus σ_a is not temperature or strain rate sensitive [13,19]. From Eq. (2), flow stress as a function of strain rate and temperature can therefore be written as Eq. (3) [13].

$$H = kT \ln(A/\dot{\varepsilon})$$ (2)

$$\sigma_f = \sigma_a + \sigma_p \left\{ 1 - \frac{kT \ln(A/\dot{\varepsilon})}{H_0} \right\}^{\frac{1}{1-m}}$$ (3)

where:

σ_a = internal stress, MPa
σ_p = Peierls stress (MPa) at T= 0 in K
k = gas constant, $1.38E^{-23}$ JK^{-1}
T = temperature in K
A = frequency factor taken as 10^8
$\dot{\varepsilon}$ = strain rate s^{-1}
H_0 = activation enthalpy associated with local barriers in J
m = material constant

Temperature rise is inherent at high strain rates owing to the short time available to conduct the heat generated during plastic work deformation in which there is no significant local heat exchange with the environment (adiabatic effect). Whereas, at low or quasi-static strain rates, the heat conduction time increases and thus, operates solely on a non-adiabatic condition because of the available time for heat conduction, leading to a lower rise in temperature [17,20]. Considering this fact, the strength model developed by Johnson-Cook [21] shows that in all cases (strain rates at 1 s^{-1}, 10 s^{-1}, 100 s^{-1}), the adiabatic stress-strain curve increased to a maximum then decreased with increasing strain. At approximately strain rate beyond 0.1 s^{-1}, adiabatic deformation dominates [17]. Whether this has significant impact on the flow stress of HSSS compared to LSSS at room temperature is a point of discussion in this paper.

3. Significance of Y/T ratio on the structural design and performance of HSSS

In engineering terms, the Y/T ratio provides the basis for measuring the deformation (strain-hardening) capacity of a material which normally increases as the static yield strength increases. This is related to the strain-hardening exponent (n), which is used to qualify the plastic deformation performance of a metal [22,23]. Usually, a higher Y/T ratio leads to a decrease in yield point elongation (Lüders Plateau) and decrease in strain-hardening exponent [22]. It means that steels with low Y/T ratios, typically in the range 0.5 to 0.85, associated with conventional low and medium strength steels have high strain-hardening exponent (extra safety margin). Whereas, modern high strength steels inherent with high Y/T ratios in excess of 0.90 exhibit low strain-hardening exponent. Hence the treatment and limitation of high Y/T ratio in design codes, **Table 2,** based on the notion that a high Y/T ratio connotes a poor fracture performance [24].

In principle, for designs based on elastic loading, i.e. stresses kept below yield, the strain-hardening characteristics beyond yield should not matter strongly in the design. This conventional approach has guided the traditional structural design methodologies where the working stress is usually taken as a proportion of the yield stress, with typical values around 60% of yield strength in normal loading and up to 80% in severe loading [5]. This concept ensures that load resistance falls within the linear region of the stress-strain curve of the component, making the Y/T ratio

irrelevant in such elastic case. More recently, plastic design concepts have been incorporated. This design approach is an additional safety precaution in steel structures in which the structure is able to yield (absorb energy) and redistribute load (work hardening) without major failure or total collapse. This design methodology has helped shape modern structural designs in defining, assessing and determining the mechanical response of steel structures under different loading conditions. In this case, the Y/T ratio becomes applicable in the post-yield behaviour of steel. Therefore, in engineering terms, the Y/T ratio can be said to be the parameter which represents the ability to withstand plastic loading and the basic measure of deformation capacity of a material [5].

Studies [7,22-27] show that the application of high Y/T ratio in HSSS has been successful in some bridge and building applications but limited in other engineering applications (especially offshore applications) due to the lack of characterisation data on their structural performance. Although the Y/T ratio only becomes relevant in the post-yield behaviour of steels, which represents the ability to withstand plastic loading and basic measure of deformation capacity, other related characteristics such as strain-hardening exponent, ductile tearing resistance, and overall global deformation are important factors to consider when considering the practicality of using high Y/T ratio as a measure of plastic strain capacity of cracked components [23].

Therefore, the successful application of HSSS with high Y/T ratio in bridges and buildings means HSSS can exploit its strength, but not rely on its ability to deform or locally yield under extreme loading.

Table 2: Treatment of Y/T ratio in accordance with various design codes taken from [1,2,4,22]

Code	Limitation (YS as proportion of UTS)	Application
API 2A-WSD	0.67 0.80*	Tubular joints, 500 MPa $< \sigma_y \leq 800$ MPa
HSE Guidance Notes (Offshore)	0.70	Tubular joints
BS 5950 (Buildings)	0.84	All components
NS 3472 (NPD) (Offshore)	0.83	All components
EC3 (Buildings, bridges and other steel structures)	0.91**/0.95	All components ($\varepsilon_{UTS} \geq 15\sigma_y/E$)
DnV (Offshore)	0.85 0.75	Except tubular joints Tubular joints ($\sigma_y >$ 500 N/mm^2)
AISC (Buildings)	0.90	Grade 50 ksi beams

*New Y/T ratio for joints provided adequate ductility is demonstrated in both HAZ and parent metal [4]

**Recommended Y/T ratio in the UK National Annex to Eurocode 3 [2]

4. Experimental methods

4.1 Materials and specimen geometries

In this paper, a program of tensile testing was developed to provide characterisation data for two high strength structural steels S690QL (WELDOX 700 EZ) and S960QL (WELDOX 960HZ) with high Y/T ratios in excess of 0.95 at a range of strain rates. The as-received delivery properties was in accordance with BS EN 10025:6 +A1 (2009) [28]. According to the standard, 690 MPa is the minimum yield strength and 940 MPa as the maximum tensile strength for nominal thickness ≤ 50 mm for S690QL. Since production route and/or chemical compositions have less effect on the tensile strength, the production process have incremental effect on the nominal yield strength when strength-to-weight ratio is important, hence the high Y/T ratio that comes with it. This is discussed in sections 1 and 5.3.

The data generated was compared with that of low strength structural steel (S235) as a representative of LSSS which has Y/T ratio < 0.80. For the purpose of easy machining, comparison and setup during quasi-static and high strain rates tension tests, flat dog-bone shaped tensile specimens were employed. The choice of flat dog-bone specimens was informed due to the recommended specimen geometry for the high speed dynamic fast jaw grip hydraulic machine. In order to make sure that the collapse load falls within the machine capacity (100 kN), the ratio between the width of the gauge area (W_a) and the shoulder width (W_s) was set at < 0.33.

Also, for a better understanding and comparison of the change of the mechanical behaviour of the materials over a range of strain rates, the aspect ratio (ratio between the width and the 3mm specimen thickness) was kept constant. The specimen geometries employed during the quasi-static and high strain rates tensile tests are shown in Figures **2 and 3,** and photographs of specimens before and after the test are shown in Figures **4 and 5** respectively. It is worth pointing out that the specimen type for the high strain rate tests requires one end to be longer, because of the testing machine requirement discussed in section 4.2. A total number of 18 specimens each were investigated for both materials. Specimens were prepared from S690QL and S960QL high strength steel plates, with load axis aligned with the rolling direction.

The choice of taking the samples in the rolling (parallel) direction was made because it is more conservative (with slightly lower differences in the yield stress) compared to samples taken in the transverse (perpendicular) direction [17]. It should be noted that the S690QL and S960QL specimens were machined from the as-received plate and supplied in thicknesses of 25mm and 60mm respectively. The grade designation stands for the following:

S – Structural Steel
690 – Minimum Yield Strength (MPa)
Q – Quenching and Tempering (Production process)
L – Low Notch Toughness Testing Temperature (Impact energy at minimum temperature).

The chemical compositions of the materials are summarized in **Tables 3a and 3b**.

Table 3a: Chemical composition of S690QL 25mm plate (%)

Element	C	Si	Mn	P	S	Ni	V	Nb	CEV
% (m/m)	0.14	0.29	1.19	0.008	< 0.002	0.084	0.031	0.016	0.42

Table 3b: Chemical composition of S960QL 60mm plate (%)

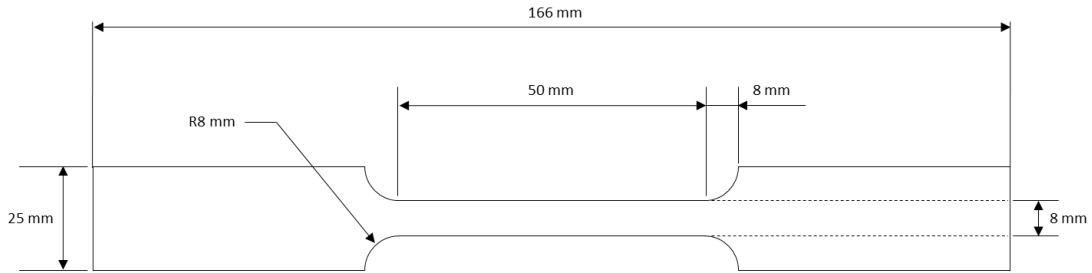| Element	C	Si	Mn	P	S	Ni	V	Nb	CEV
% (m/m)	0.16	0.21	1.39	0.008	< 0.002	0.077	0.021	0.013	0.55

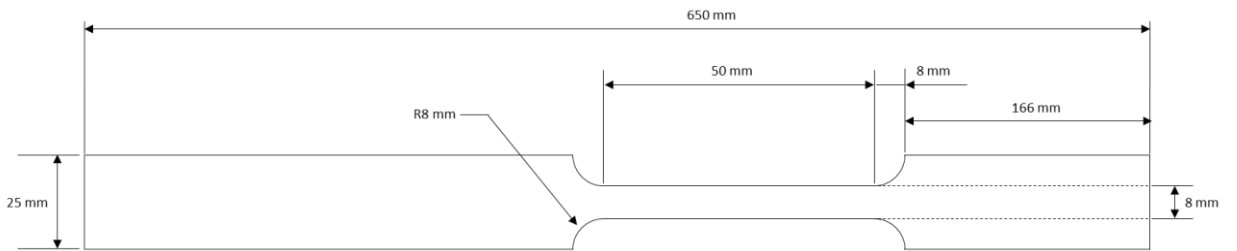**Figure 2:** Quasi-static tensile test specimen geometry. Courtesy of TWI Ltd.

Figure 3: Dynamic tensile test specimen geometry for strain rate above 4 s^{-1}.
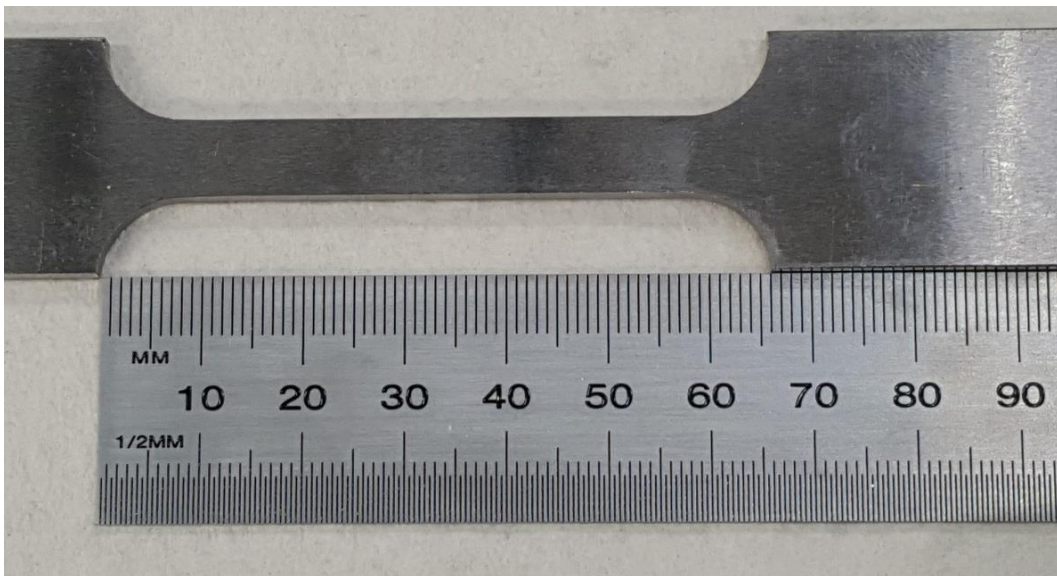Courtesy of TWI Ltd.

Figure 4: Photograph of specimen before test. Courtesy of TWI Ltd.
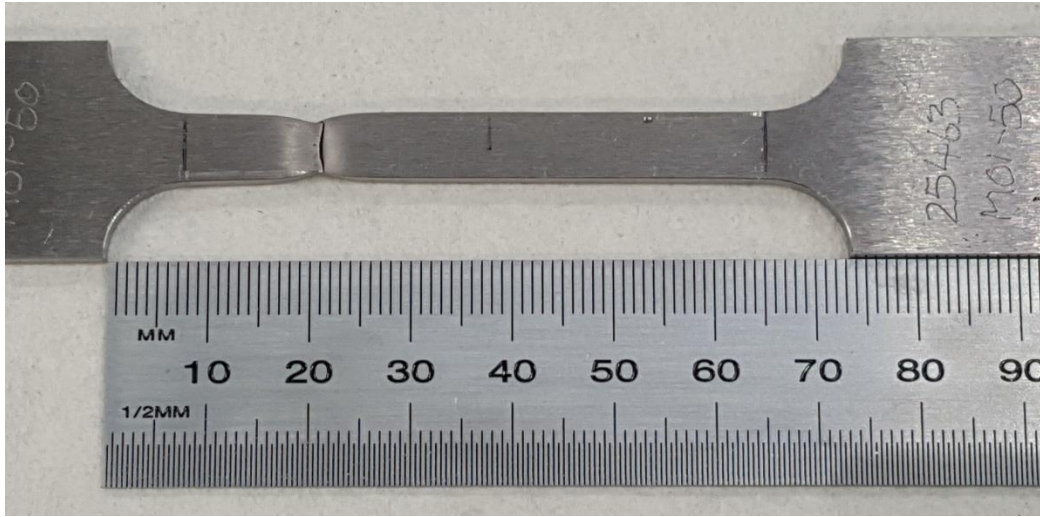
Figure 5: Photograph of specimen after test. Courtesy of TWI Ltd.

4.2 Setup and test procedures

Dynamic tests require a special machine capable of high speed loading and data recording along with skilled and experienced personnel for the experimental procedures and setup. This has made dynamic testing over the years very expensive and, as such, has made quasi-static testing conditions generally accepted for design purposes. This is why most offshore and marine structures such as ships and fixed structures are often designed for quasi-static loading conditions despite that there are occasions when dynamic loading such as impact from ship collision or dropped objects could affect the response of the structure. It is therefore imperative to quantify the mechanical response in terms of in-service loading conditions since structures do not always operate under quasi-static loading conditions. To bridge this gap, tests were carried at quasi-static and in-service loading rate scenarios, especially those experienced by offshore cranes **(Table 1)**. Instron Machine B909 was employed for tests from quasi-static up to 4 s^{-1} strain rates with the use of extensometer and load cell to measure the stress-strain characteristics of the material at room temperature. Tests above 4 s^{-1} strain rates were carried out at room temperature on an Instron VHS 160 Dynamic Test Machine. The machine is a special dynamic testing machine with capacity of 100 kN with speed up to 20 m/s, utilising advanced servohydraulic and control technologies alongside patented FastJaw gripping techniques. The gripping techniques require one end of the flat tensile specimen longer than the other in order to give room for travel. All tests were performed at TWI, Cambridge.

To maintain accuracy and precision at strain rate above 10 s^{-1}, high speed recording equipment is required. The use of a Digital Image Correlation (DIC) system has proven to be a suitable option for the measurement of the strain profile experienced by the specimen under high loading conditions. Since the purpose of the test is to determine the effects of high loading rates in terms of strain rate, DIC was employed with the VHS high speed test machine. The DIC system is calibrated to measure within a certain measuring volume which takes a trigger pulse from the VHS test machine to start the camera and data logger. The DIC system required a high speed camera to capture about 70,000 frames/sec number of data points along the gauge length of the specimen. The camera setup (field of view used, frame rate and standoff distance) all contribute to the number of data points. The setup of the test

machine and DIC system is shown in Figures **6 and 7,** respectively. For the purpose of this paper emphasis will be made on tests from quasi-static up to 100 s^{-1} strain rates and at ambient temperature.

In order to achieve the required overall precision, it is noteworthy that the experience of the technician played an important role. Whilst the use of DIC at high loading rate required skilled and experienced personnel, the test-setup and accuracy at strain rate below 10 s^{-1} also require a well calibrated machine, experienced personnel and accurate stress-strain measurements (with the use of an extensometer attached to the specimen gauge length). At the end of each test, both cross-section reduction and gauge length extension were measured.
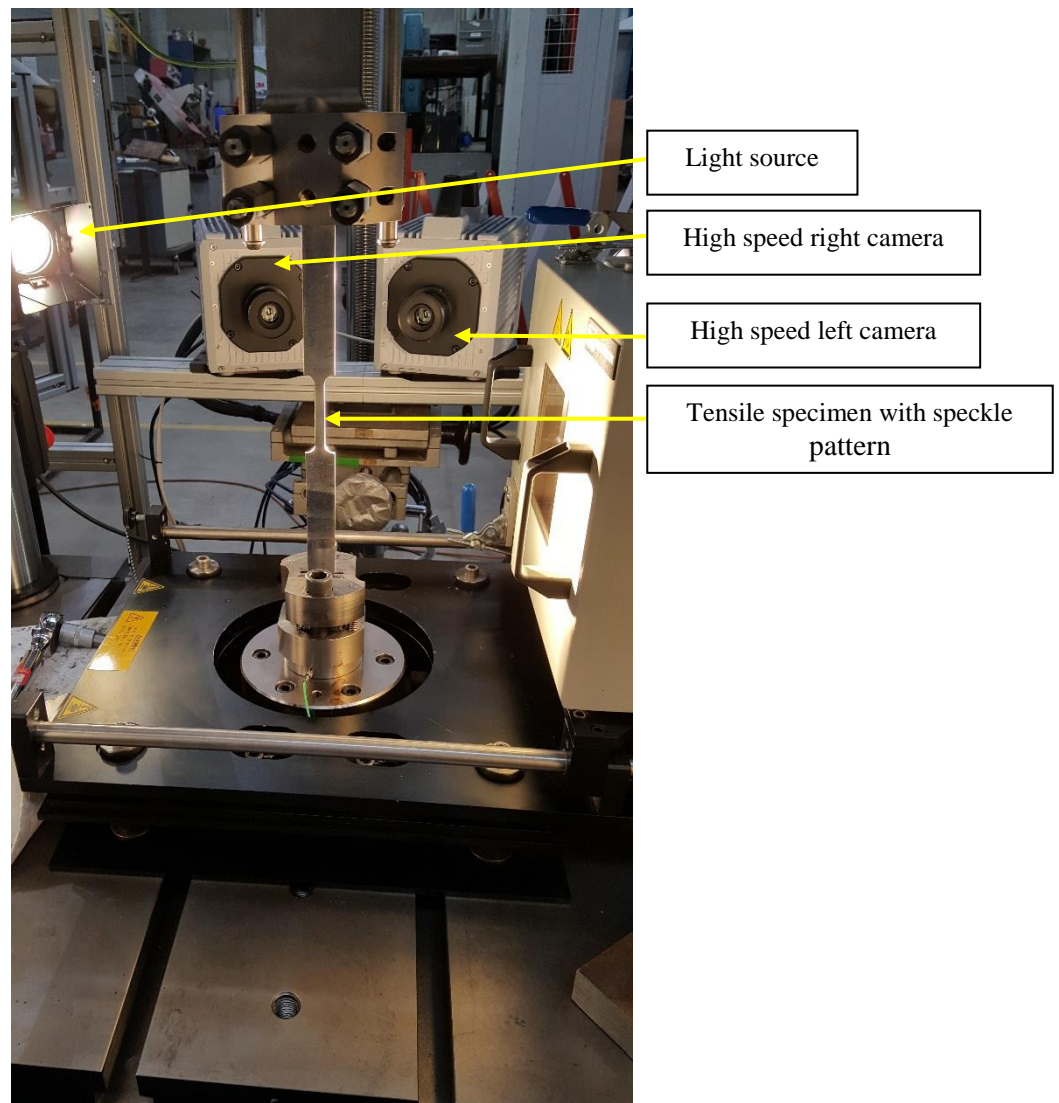
Figure 6: DIC system setup with the VHS test machine with view from behind (facing the camera). Courtesy of TWI Ltd.
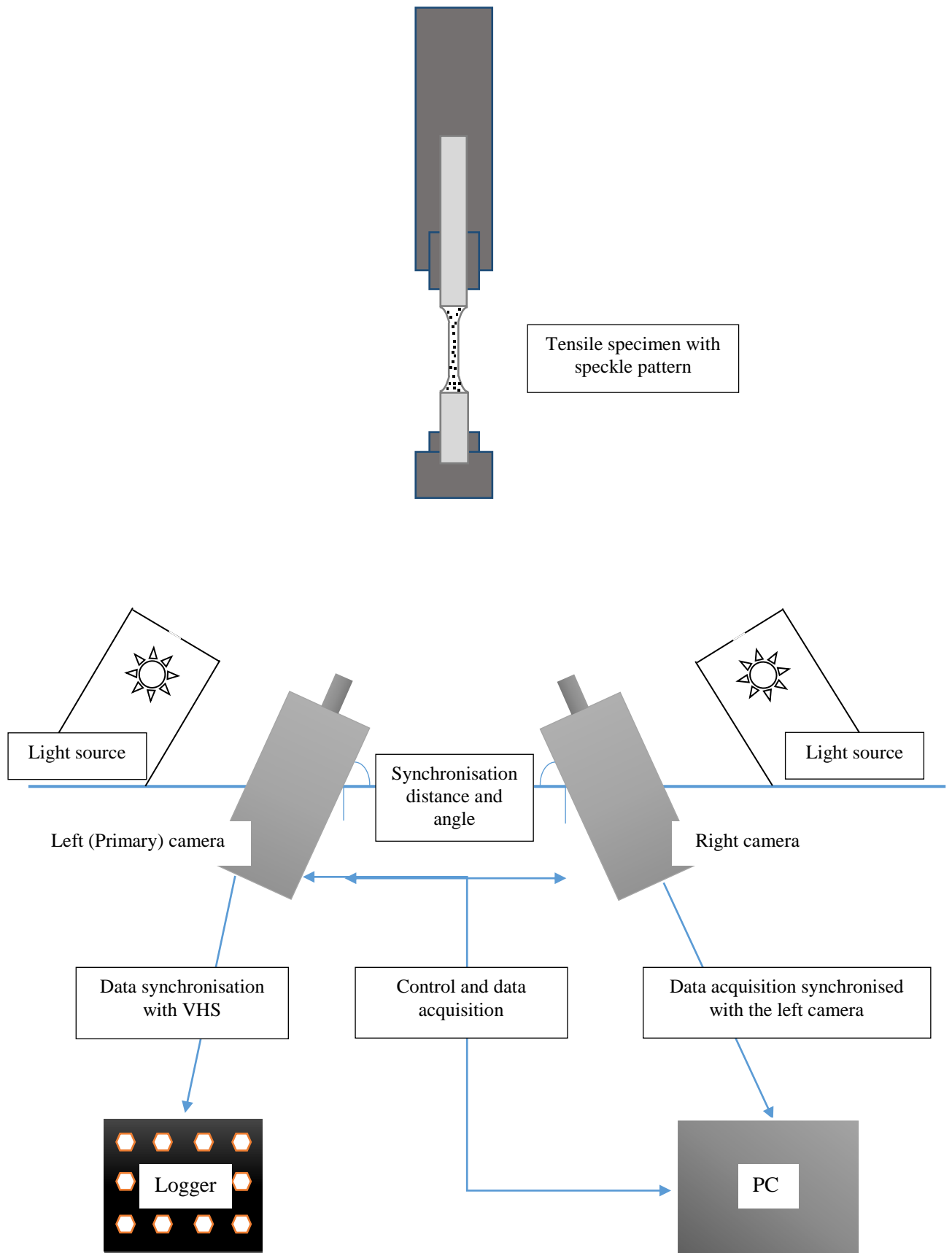
Figure 7: A simple schematic representation of the DIC setup and framework with the VHS machine. Courtesy of TWI Ltd.

5. Results and Discussion

5.1 Initial uniaxial tensile test results on S690QL at quasi-static strain rate

Initial uniaxial tensile tests at room temperature were carried out to determine how material geometry and/or cross-sections affect the overall plastic deformation (uniform and localised) under quasi-static condition as shown in Figure **8** using designations M01 and M02 to represent samples with cross sectional areas 24 mm^2 and 38 mm^2, respectively. Within the elastic limit, no notable change is observed but a significant difference is noticed in the plastic work. Although for low cross sectional area (M01) a reduced value of about 20% in strain-hardening exponent (n) compared to high cross sectional area (M02) is obtained as shown in **Table 4**, there is a similarity in the plastic work shape prior to necking. A low cross section gave enhanced percentage reduction in area after necking (non-uniform plastic work deformation or local elongation). The Y/T ratio in **Table 4** is taken as the ratio of the 0.2% proof stress and ultimate tensile strength from engineering stress-strain curve. Also, the linear fit from the logarithmic relationship of the true stress-strain curve ($\sigma=K\varepsilon^n$) where σ is the stress, ε is the strain, n is the strain-hardening exponent and K is the strength coefficient represents the value of the strain-hardening exponent used for the analysis. These definitions and approach to determining the values of Y/T ratio and n have been employed in this paper.

The result means that elongation and reduction in area is a measure of different responses in the mechanical behaviour of a material and should not be generalized as a means of measuring ductility. Uniform plastic elongation is highly influenced by plastic work hardening, whereas reduction in area is a representation of a local plastic work deformation before fracture. As such, reduction in area is influenced by the necking process and is the most structure-sensitive ductility factor in detecting quality changes in a material behaviour after necking **[29,30]**. Therefore, the extent of plastic work deformation does not only depend on the strain-hardening curve but also depends on the specimen geometry and the shape (cross sections) prior to necking formation.

Table 4: Effect of specimen geometry on strain-hardening exponent (n)

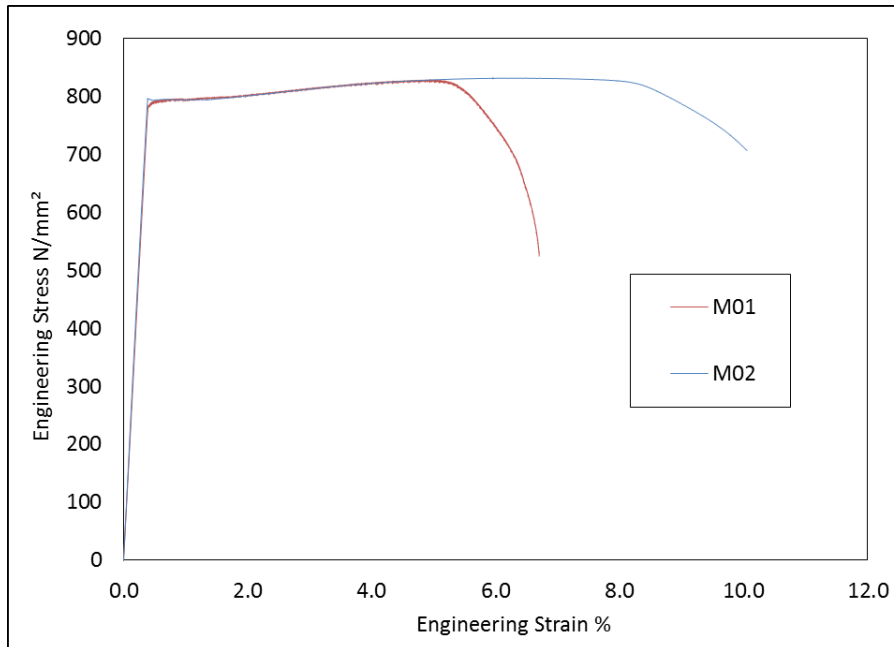| Specimen No	CSA[*]	Strain-hardening exponent (n)	Y/T Ratio	Strain Rate (s^{-1})
M01	24 mm^2	0.044	0.956	2x10^{-4}
M02	38 mm^2	0.053	0.955	2x10^{-4}

[*]CSA is cross sectional area

Figure 8: Effect of specimen geometry on S690 at quasi-static loading condition. Courtesy of TWI Ltd.

Specimens with a cross sectional area of 24 mm^2 are used for all subsequent tests so that comparisons could be made at different strain rates, but conclusions based on absolute values cannot be drawn.

5.2   *Characterisation of S690QL and S960QL*

Based on the initial tests, comprehensive uniaxial tensile tests were performed to characterise the mechanical behaviour of S690QL and S960QL high strength structural plates at a range of strain rate up to 100 s^{-1}. Strain rates from quasi-static (QS) (0.0002 s^{-1}) to high/dynamic (~100 s^{-1}) extend over the primary strain rate range encountered in an offshore or marine in-service conditions, **Table 1**. Yield stress is defined as the 0.2% proof strength for all samples, to enable the yield-to-tensile ratio to be determined. Information regarding offshore structures in-service scenarios under normal and high strain rate conditions revealed that time at maximum force could be around 1.3 s and 0.25 s, respectively **[11]**. For the tensile tests carried out, the corresponding time to maximum force and fracture at 1 s^{-1} strain rate (the critical strain rate for offshore cranes) falls around 0.08 s and 0.12 s, respectively. This is slightly lower but similar to those given by Walters et al. **[11]** for offshore structures. Based on this understanding more emphasis will be made for strain rates from QS to 4 s^{-1}, however discussion will still include the strain rate at 100 s^{-1}.

It is worth noting that the measurement of load signal at 100 s^{-1} was challenging due to the requirements for accuracy and precision. DIC was employed for this purpose and the results from tests at 100 s^{-1} strain rate are presented in Figures **9, 10 and 11** for LSSS (S235) and HSSS (S690 and S960), respectively**.** The raw data represents the load cell signal syncronised with the reading from the DIC. The strain measurement was taken from the DIC, which records the strain profile on the sample. Due to the imbalance between the internal and external forces during high strain problems, the load signal was noisy as a result of stress wave propagation developed during the test. To reduce the noise in the data, averaged data using moving average

technique in matlab was employed and, this was used to quantify the effect of strain rate at 100 s⁻¹ for the three materials under consideration.
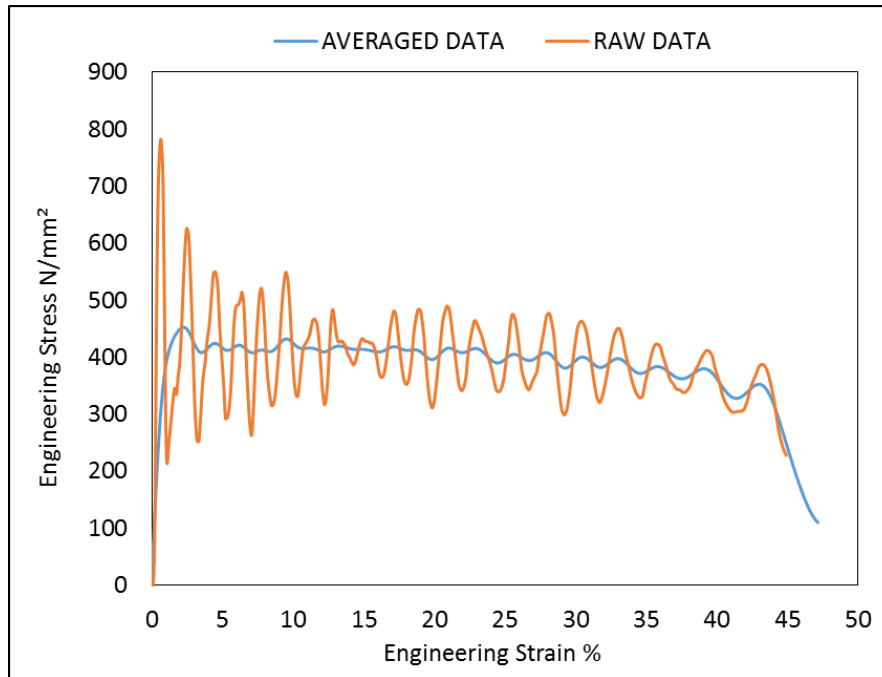

Figure 9: S235 result at strain rate of 100 s⁻¹. Courtesy of TWI Ltd.
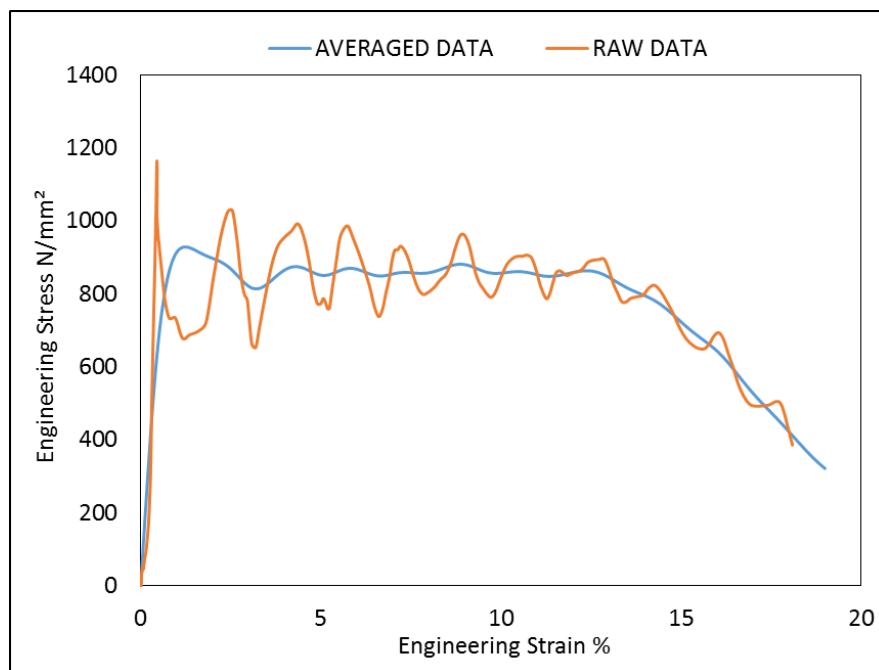

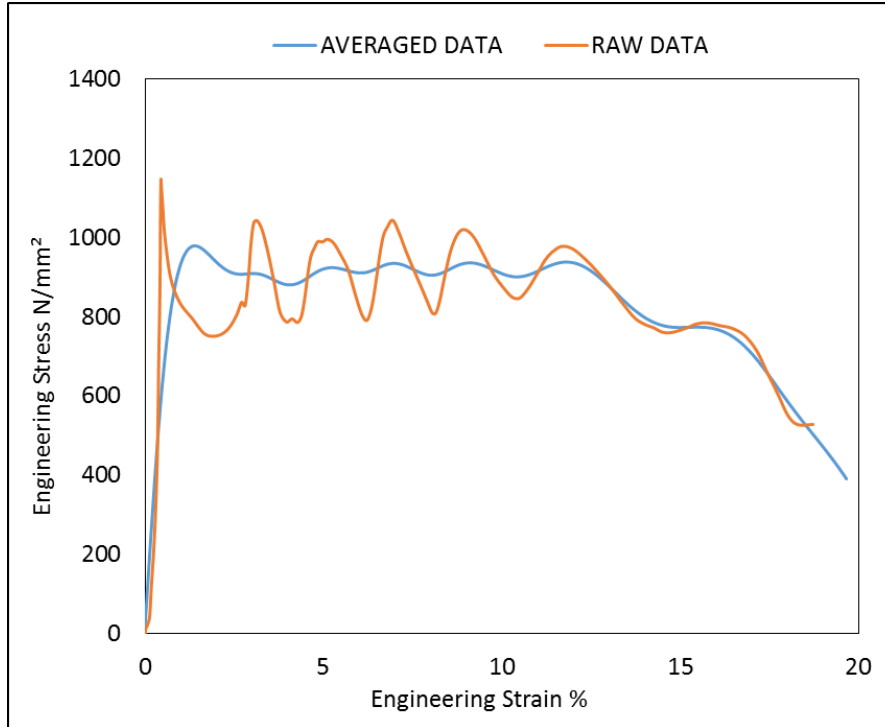**Figure 10**: S690 result at strain rate of 100 s⁻¹. Courtesy of TWI Ltd.

Figure 11: S960 result at strain rate of 100 s^{-1}. Courtesy of TWI Ltd.

The results show that the dynamic amplification as a result of strain rate effect on the yield stress of LSSS with Y/T ratio < 0.8 (S235) is high. The degree of sensitivity of HSSS with Y/T ratio > 0.95 (S690QL and S960QL) is relatively unaffected by the strain rate effect. About 66% amplification was observed on the yield stress of low strength steel (S235) from quasi-static to 100 s^{-1} strain rates. This is an equivalent of about 1.66 dynamic increase factor as shown in Figure **12**. On the other hand, this effect (strain rate sensitivity) is less notable on the HSSS (S690QL and S960QL) whose dynamic amplification effect on yield stress from QS to 100 s^{-1} is less than 10%. This is due to the fact that the degree of sensitivity of steel decreases with increasing nominal yield strength. For this reason, the metallurgical and production techniques used to achieve the strength level of S690QL and S960QL were studied and discussed in the next section. Also noted is the high sensitivity of the strain at the initiation of strain hardening. This shows that the degree of sensitivity is high at 0.2% proof stress or zero plastic strain. Since yield strength is linearly related to the logarithm of the strain rate **[10]**, it follows that a semi-logarithmic graph can be used to represent the flow stress increase factor dependence on dimensionless strain rate, Figures **13 and 14**, using Eq. (4) **[17,21]**. The sensitivity decreases as the plastic strain increases at ambient temperature.

$$F = 1 + C \ln(\dot{\varepsilon}^*) \qquad (4)$$

where:

F   = flow stress increase factor σ_d/σ_0

C   = sensitivity parameter

$\dot{\varepsilon}^*$ = dimensionless strain rate $\dot{\varepsilon}_p / \dot{\varepsilon}_0$
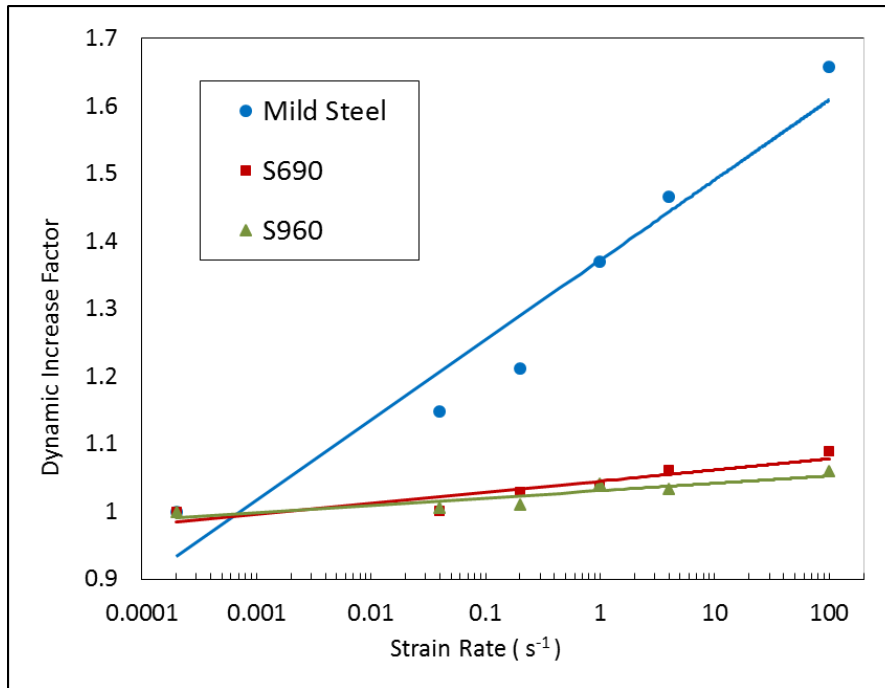
Figure 12: The effect of strain rate on the yield true stress of S235, S690 and S960 from QS to 100 s^{-1}. Courtesy of TWI Ltd.
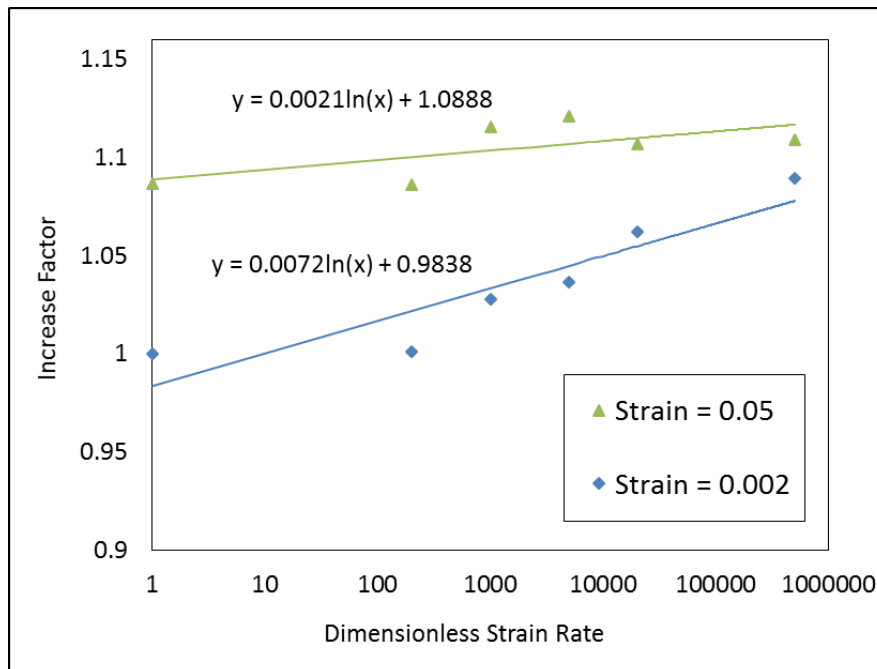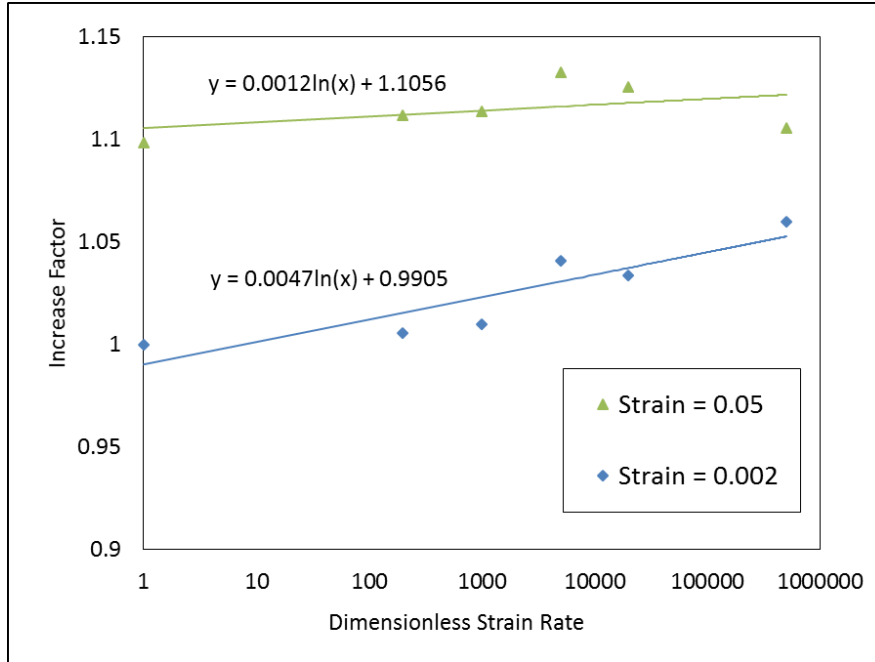

Figure 13: Flow stress increase factor (σ_d/σ_0) dependence on the dimensionless strain rate ($\dot{\varepsilon}_P/\dot{\varepsilon}_0$) for S690. Reference strain $\dot{\varepsilon}_0$ taken as 2 x 10^{-4} s^{-1}. Courtesy of TWI Ltd.

Figure 14: Flow stress increase factor (σ_d/σ_0) dependence on the dimensionless strain rate ($\dot{\varepsilon}_P/\dot{\varepsilon}_0$) for S960. Reference strain $\dot{\varepsilon}_0$ taken as 2 x 10^{-4} s^{-1}. Courtesy of TWI Ltd.

The Y/T ratio only becomes relevant in the post-yield behaviour of steels, which represents the ability to withstand plastic loading and as a measure of deformation capacity. Designs based on elastic loading, i.e. stresses kept below yield, the strain-hardening characteristics beyond yield should not matter strongly in the design. Figure **15** shows that the Y/T ratio for S235 grade mild steel increased from around 0.7 at quasi-static loading rates, steadily up to around 1 at 100 s^{-1}. The S690 and S960 Y/T ratio kept fairly constant, ranging between 0.95 and 1 throughout the strain rate range tested. Also, since the strain-hardening exponent (*n*) determines the plastic deformation performance of steel, the strain-hardening exponent was determined using the power law approach ($\sigma=K\varepsilon^n$). A downward trend was observed on the *n* value of S235 as the strain rate increases from QS to 100 s^{-1}. For the HSSS (S690 and S960), *n* kept fairly constant at up to 4 s^{-1} strain rate but dropped at 100 s^{-1}, Figure **16**. A relationship between Y/T ratio and *n* has been developed **[23-24]**. The expression in Eq. (5) provides a conservative lower bound fit for calculating *n* from Y/T ratio, Figure **17,** where *N* represents strain-hardening exponent. From Figure **17**, it is important to point out that the materials may look the same, but they are not of the same tensile properties. S690QL, delivered in 25 mm thickness has nominal yield strength of about 817 MPa and 0.96 Y/T ratio, whereas and S960QL delivered in 60 mm has nominal yield strength of about 906 MPa and Y/T ratio 0.95. This is important to point out because it would help the users to have clear information about the tensile performance of these steel grades with varying thickness delivery conditions.
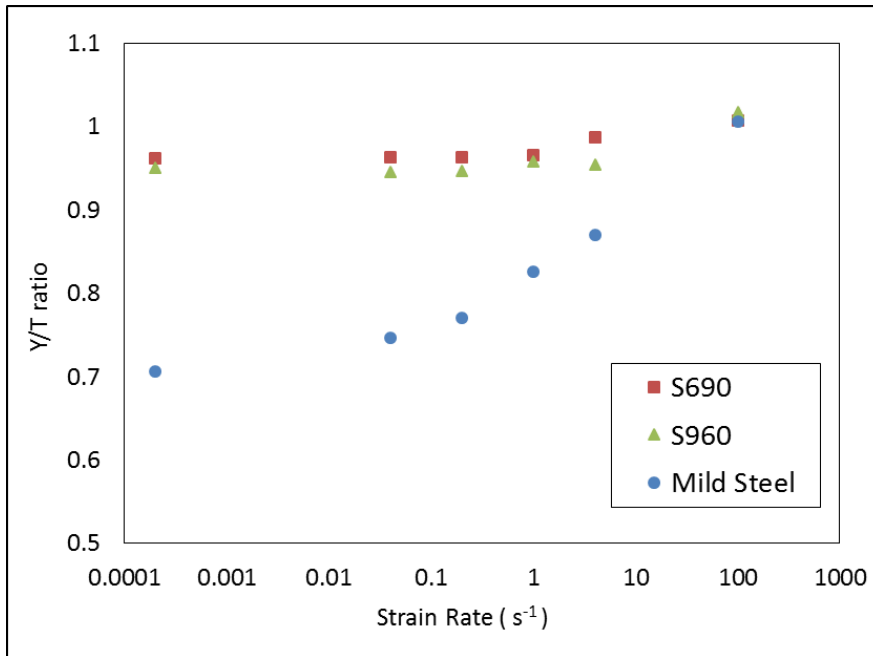
$$N = 0.3[1 - (Y/T)] \qquad\qquad (5)$$

Figure 15: The effect of strain rate on the Y/T ratio of mild steel and high strength steels. Courtesy of TWI Ltd.
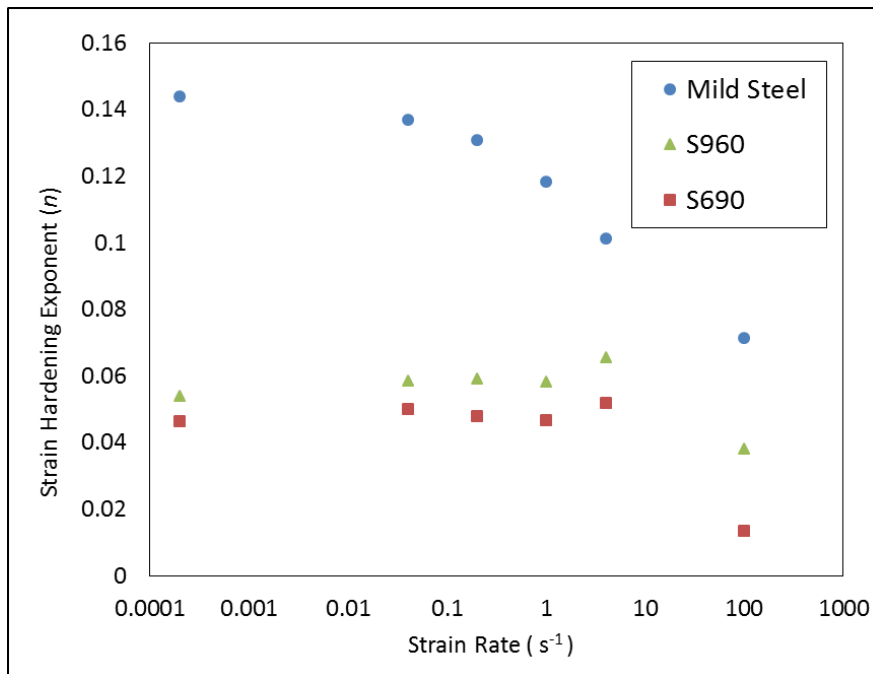

Figure 16: Effect of strain rate on the strain-hardening exponent (*n)* of LSS (mild steel) and HSSS. Courtesy of TWI Ltd.
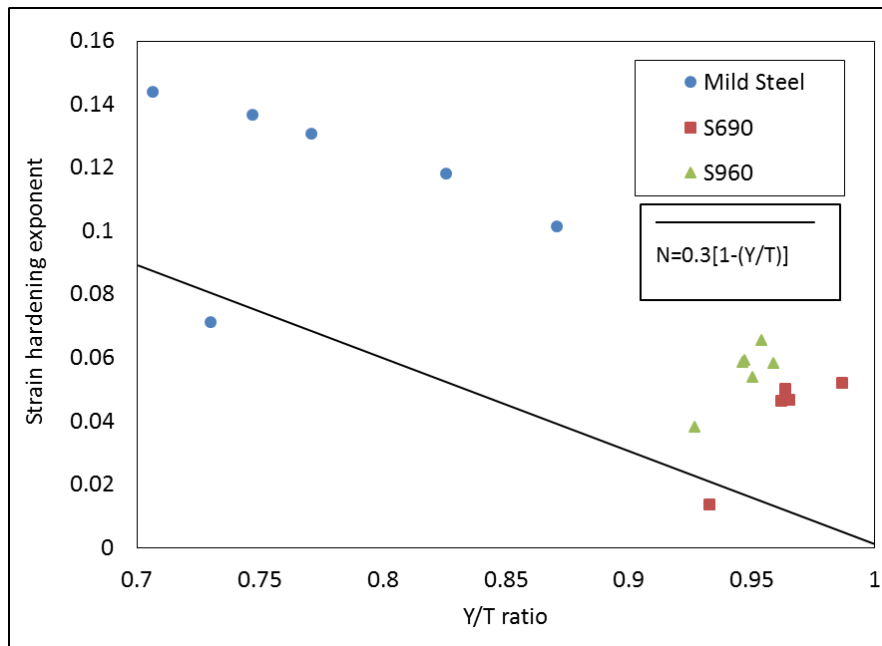
Figure 17: A conservative lower bound fit for calculating strain hardening exponent (*N*) from Y/T ratio using SINTAP approach, Eq. (5) **[24]**. Courtesy of TWI Ltd.

The flow stresses of S690QL and S960QL from QS up to 4 s^{-1} are shown in Figures **19 and 20**, respectively, with increased ductility at moderately high strain rates. This is compared with mild steel (S235) as shown in Figure**18**. The effective plastic strain here is the total true strain minus the recoverable strain (ratio of true stress and elastic Young Modulus). It is worth pointing out that, from Figures **19 and 20**, the material shows peak effect as the strain rate increases, and this is not considered in the analysis as 0.2% proof stress was taken as the yield strength for all.
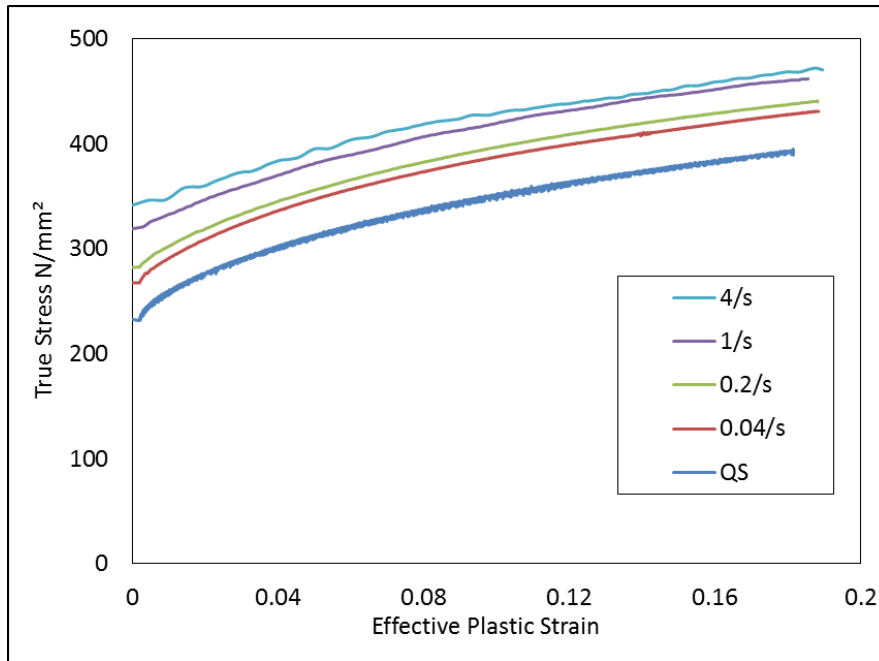
Figure 18: Flow stress for mild steel (S235) generated up to 4 s^{-1} strain rate. Courtesy of TWI Ltd.
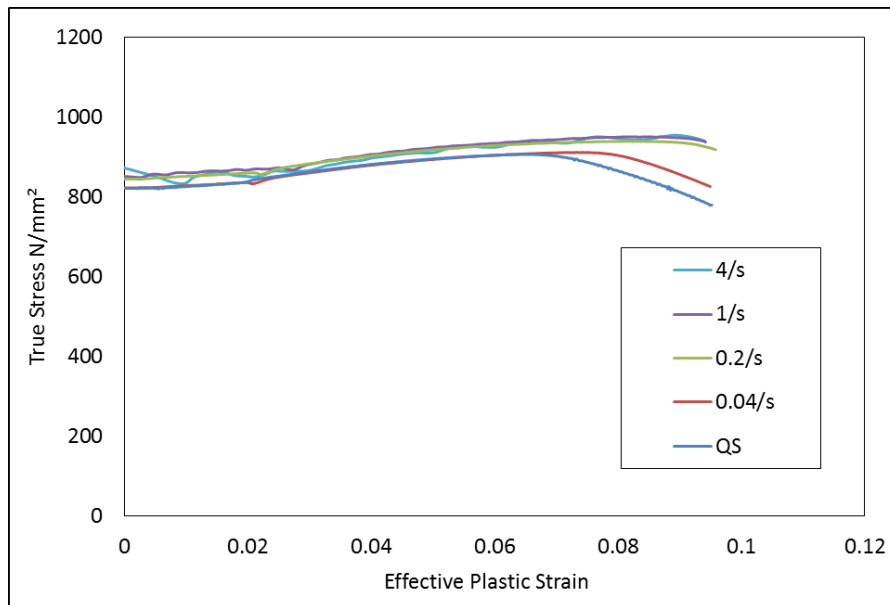

Figure 19: Flow stress for S690QL generated up to 4s^{-1} strain rate. Courtesy of TWI Ltd.
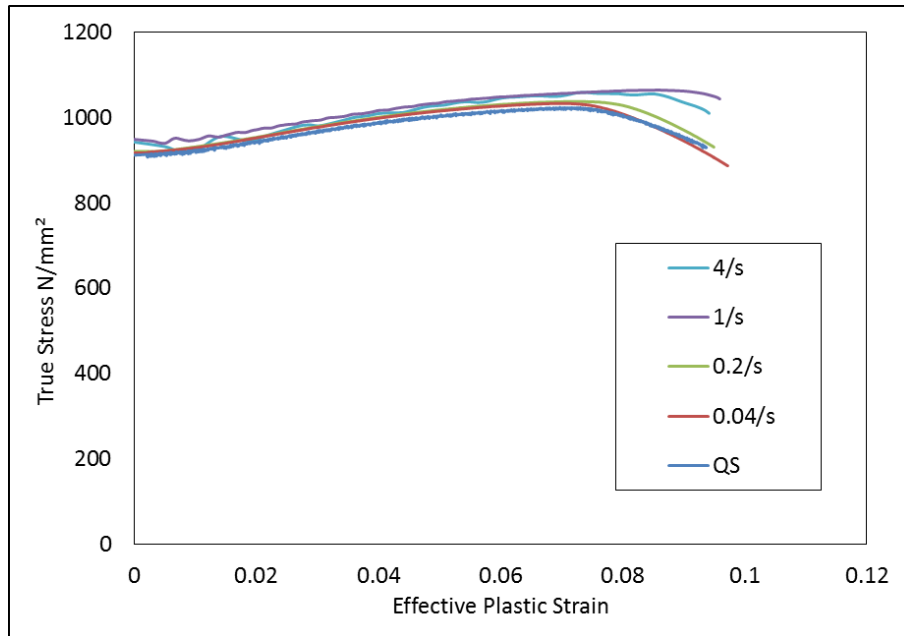
Figure 20: Flow stress for S960QL generated up to 4s^{-1} strain rate. Courtesy of TWI Ltd.

5.3 Metallographic Examination

Traditionally, alloying elements such as carbon and manganese added to steel increase nominal yield strength, with detrimental effects on the fabrication properties of steels, in particular, weldability. To avert this effect, carbon contents in modern steels are limited, along with a high degree of cleanliness and typical sulphur and phosphorus levels of < 0.005% and < 0.010% respectively implemented for good toughness and through-thickness homogeneity [25]. Modern production routes such as Quenched and Tempered (QT), Thermomechanically Controlled Rolled (TMCR) or Accelerated Cooled (AC/TMCP) were developed to promote fine-grained and homogeneous structures with higher strength, thereby improving the combination of strength level and toughness in modern and high performance HSSS. These production processes and/or compositions have less effect on the ultimate tensile strength but an incremental effect on the nominal yield strength, and consequently high Y/T ratio. The increase in nominal yield strength of steel predominantly achieved via alloying and heat treatment, affect the degree of sensitivity to strain rate because of the fine-grain size achieved during the process. Metallographic examination was carried out to determine to some extent the effect of grain size on the strain rate sensitivity. The metallographic examination shows a variation in grain size of the three materials (S235, S690 and S960) under consideration. It is seen that the examination from S235 micrograph, Figure **21,** shows coarse grain size and inclusions as a result of large concentrations of impurities (high sulphur content). On the other hand, S690QL and S960QL showed a fine-grained size structure and high degree of cleanliness with typical sulphur and phosphorus levels of < 0.002% and < 0.009%, Figures **22 and 23**. There is no doubt that the tempered martensite structure, such as achieved in S690QL and S960QL quenched after austenising above room temperature and rapid cooling in water, would have a different degree of rate sensitivity compared to steel grades produced via a Normalised (N) heat treatment route, heated slightly above the temperature where its austenite totally changes to a ferritic-perlitic structure followed by slow cooling. It should be noted that the

micrographs shown in Figures **21 to 23** refer to as as-received grain size material properties.

The grain size was determined according to ASTM E112 **[31]**, as given in **Table 5**. From the results, the grain size varies from 0.021 mm to 0.008 mm; a larger grain size was observed in S235 while S960 has the smallest. Obviously, the production routes have an effect on the grain size and the grain size influences the strength level. Therefore, it can be said that among other factors the degree of strain rate sensitivity depends on the production routes, chemical compositions and consequently a finer-grained structure with less sensitivity is recorded when the nominal yield strength increases.

Table 5: Calculated grain size according to ASTM E112 **[31]**

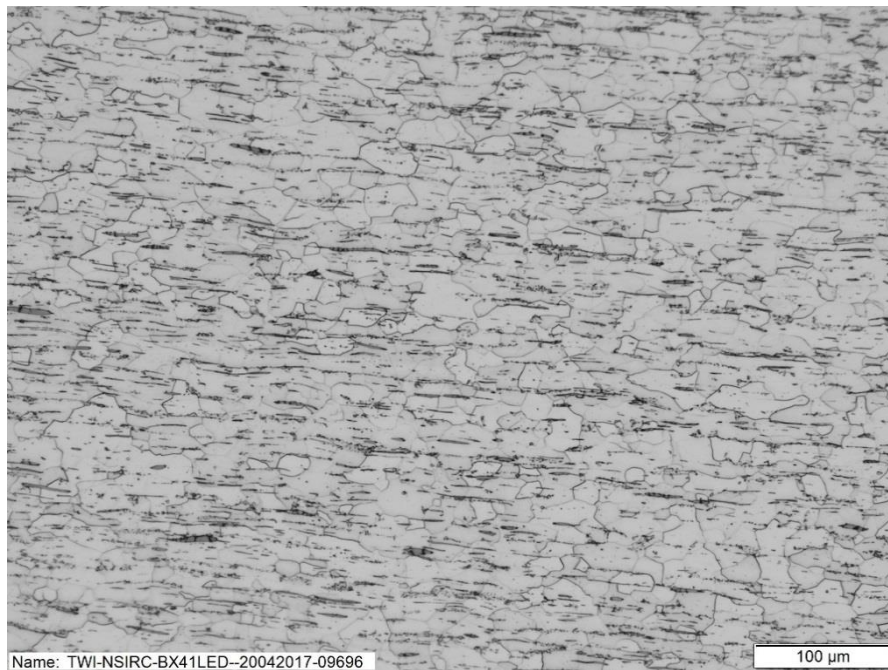| Materials	ASTM grain size	Mean grain diameter (mm)
S235	8	0.021
S690	10	0.011
S960	11	0.008

Figure 21: Micrograph of Mild Steel (S235) etched with 2% Nital. Courtesy of TWI Ltd.
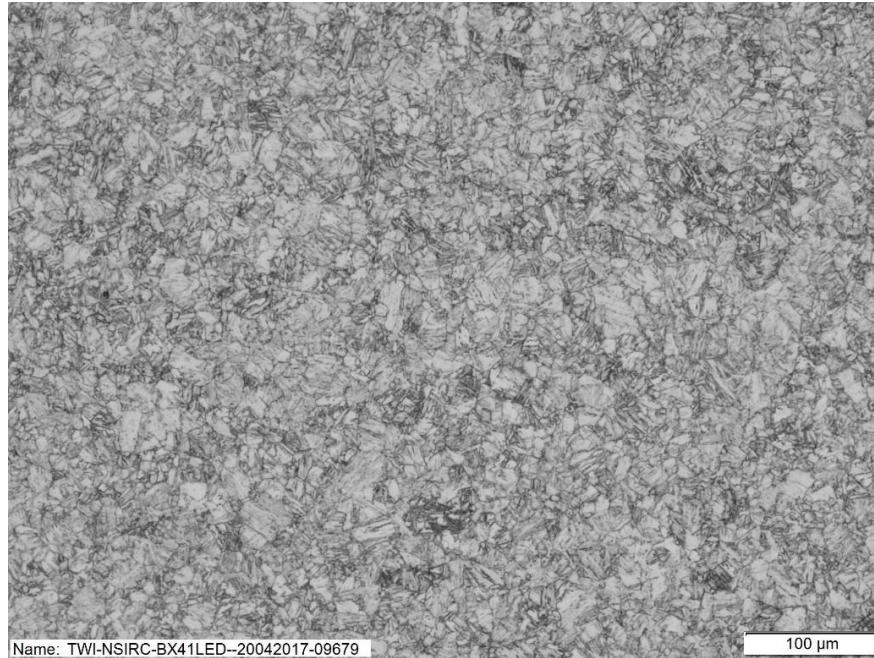
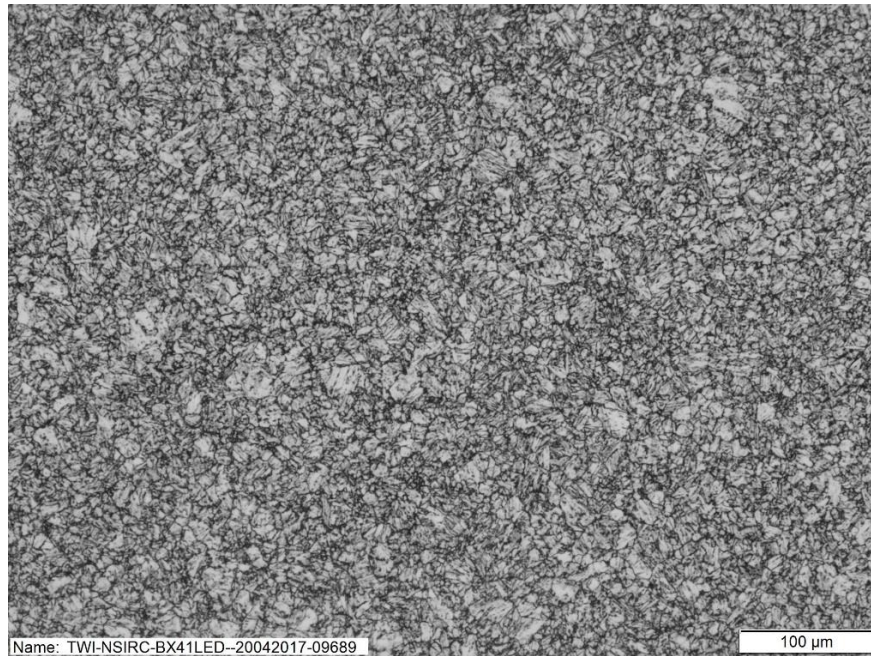**Figure 22:** Micrograph of S690 etched with 2% Nital. Courtesy of TWI Ltd.

Figure 23: Micrograph of S960 etched with 2% Nital. Courtesy of TWI Ltd.

6. Conclusions and Recommendations

The effect of strain rate on the tensile properties of HSSS compared to LSSS has been studied. Major findings include the following:

- The high strength structural steels with Y/T ratio > 0.90 are less sensitive to the effect of strain rate when compared to the LSSS structural steels with low Y/T ratio < 0.8.
- The extent of plastic work deformation does not only depend on the strain

hardening curve but also depends on the specimen geometry and the shape (cross-section) prior to necking formation.

- The yield stress for S235 mild steel grade increased by about 66% from quasi-static to 100 s^{-1} strain rate. The effect of strain rate up to 100 s^{-1} on the yield stress of S690QL and S960QL moderately increase to about 9% and 6%, respectively.

- In terms of strain-hardening exponent (n), the value of n for S235 decreases as the strain rate increases whereas for S690 and S960, n kept fairly constant at up to 4 s^{-1} strain rate but decrease drastically at 100 s^{-1}.

- Finer-grained size microstructures were associated with a reduced degree of strain rate sensitivity. The degree of strain rate sensitivity in the tensile properties therefore depends on the production routes, chemical compositions and microstructure.

- The strain rate effect on the HSSS at strain rates from 4 s^{-1} to 100 s^{-1} should be characterised with a larger data set to increase confidence in the trends within this loading rate range.

- The tensile performance of HSSS under quasi-static conditions gives a reasonably accurate prediction of its behaviour under high loading up to 4 s^{-1} strain rate without requiring any specialist tensile testing for its characterisation.

- In the absence of high strain rate test data, quasi-static test data of S690QL and S960QL can be used to characterise its tensile behaviour up to 4 s^{-1} strain rate at room temperature.

As the experimental tensile test results show that S690QL and S960QL are relatively unaffected by the effect of structural loading rate from quasi-static up to 100 s^{-1} strain rates (typical strain rate that offshore or marine structures may be subjected to), fracture toughness values at different structural loading and temperature conditions encountered in primary offshore structural applications would help to better understand the mechanical response and performance of these materials even in the presence of flaws. Further research is required to establish the Ductile-to-Brittle Transition Curve (DBTC) of these materials (S690QL and S960QL) where a shift from the upper shelf to lower shelf could be unsafe. To this end, ongoing experimental fracture toughness investigation is expected to play an important role in predicting the mechanical behaviour of high strength structural steels with high yield-to-tensile ratio in addition to the finite element analysis and design optimisation.

References

[1] Eurocode 3, Design of steel structures: Part 1-12, Additional rules for the extension of EN 1993 up to steel grades S 700, 2007.

[2] *UK National Annex to E*urocode 3, Design of steel structures: Part 1-12, Additional rules for the extension of EN 1993 up to steel grades S 700, 2007.

[3] J. Billingham, J. V. Sharp, J. Spurrier, P. J. Kilgallon, Review of the performance of high strength steels used offshore, HSE research report 105, 2003 (URL http://www.hse.gov.uk/research/rrpdf/rr105.pdf).

[4] API 2A-WSD, Planning, designing, and constructing fixed offshore platforms – Working Stress Design, American Petroleum Institute recommended practice 21st Edition, 2014.

[5] J. Healy, J. Billingham, C. Billington, H. Bolt, Design implications of the high yield to ultimate ratio of high strength steels in offshore engineering, OMAE1995, vol. 3: Materials Engineering, ASME (1995) 271-277.

[6] R. J. Dexter, M. Ferrell, Optimum Weld-Metal Strength for High-Strength Steel Structures, ATLSS Report No. 95-08, Sponsored by Ship Structure Committee, U.S. Coast Guard, July 1995 (URL https://preserve.lehigh.edu/engr-civil-environmental-atlss-reports/210).

[7] H. Y. Ban, G. Shi, A review of research on high-strength steel structures, Structures and Buildings, Proceeding of the Institution of Civil Engineers, (2017). (URL http://dx.doi.org/10.1680/jstbu.16.00197)

[8] K. Wallin, Fracture Toughness of Engineering Materials – Estimation and Application, EMAS Publishing, Birchwood Park, Warrington, UK, 2011.

[9] Bomel Limited, The behaviour of carbon steels at high strain rates and strain limits, Offshore Technology Report (OTO 1999/018), HSE, 1999 (URL http://www.hse.gov.uk/research/otopdf/1999/oto99018.pdf).

[10] P. H. Francis, T. S. Cook, A. Nagy, The effect of strain rate on the toughness of ship steels, Ship Structure Committee Report (SSC-275) under project SR-1231, 1978 (URL http://www.shipstructure.org/pdf/275.pdf).

[11] C. L. Walters, J. Przydatek, Relating structural loading rate to testing rate for fracture mechanics specimens, OMAE2014–23962, Vol 5: Materials Technology; Petroleum Technology, ASME (2014) V005T03A028, http://dx.doi.org/10.1115/OMAE2014-23962 (URL http://proceedings.asmedigitalcollection.asme.org/proceeding.aspx?articleid=1911751).

[12] C. S. Wiesner, H. MacGillivray, Loading rate effects on tensile properties and fracture toughness of steel, paper presented at TAGSI Seminar – Fracture, Plastic Flow and Structural Integrity (dedicated to Sir Alan Cottrell in the year of his Eightieth Birthday), held at TWI, Cambridge, UK, 1999 (URL http://www.twi-global.com/technical-knowledge/published-papers/loading-rate-effects-on-tensile-properties-and-fracture-toughness-of-steel-april-1999/).

[13] F. M. Burdekin, W, Zhao, Y. Tkach, C. S. Wiesner, W. Xu, The effects of dynamic loading on structural integrity assessments, HSE research report 208, 2004 (URL http://www.hse.gov.uk/research/rrpdf/rr208.pdf).

[14] B. Burgan, Elevated temperature and high strain rate properties of offshore steels, Offshore Technology Report (OTO 2001/020), HSE, 2001 (URL http://www.hse.gov.uk/research/otopdf/2001/oto01020.pdf).

[15] J. Choung, W. Nam, J-Y. Lee, Dynamic hardening behaviours of various marine structural steels considering dependencies on strain rate and temperature, Marine Structures vol. 32, (2013) 46-67, https://doi.org/10.1016/j.marstruc.2013.02.001 (URL www.sciencedirect.com/science/article/pii/S0951833913000154).

[16]   N. NagarajaRao, M. Lohrmann, L. Tall, Effect of strain rate on the yield stress of structural steel, ASTM Journal of Materials, vol. 1, No. 1, Publication No. 293 Fritz Laboratory Reports, Paper 1684 1966 (URL http://preserve.lehigh.edu/engr-civil-environmental-fritz-lab-reports/1684).

[17]   D. Breuk, Flow stress and ductile failure at varying strain rates, ISBN 90-9016534-7, 2003.

[18]   J. D. Campbell, W. G. Ferguson, The temperature and strain-rate dependence of the shear strength of mild steel, Philosophical Magazine, vol. 21, iss.169, (1970) 63-82, http://dx.doi.org/10.1080/14786437008238397 (URL http://www.tandfonline.com/doi/pdf/10.1080/14786437008238397?needAccess=true).

[19]   J. W. Morris, Overview of dislocation plasticity, Introduction to Materials Science vol. i, (2007) 1–36 (URL http://www.mse.berkeley.edu/groups/morris/MSE205/Extras/dislocation plasticity.pdf).

[20]   A. Trondl, D-Z. Sun, Modelling of strain rate dependence of deformation and damage behaviour of HSS and UHSS at different loading states, 10th European LS-DYNA Conference, Würzburg, Germany, 2015 (URL http://www.dynalook.com/10th-european-ls-dyna-conference/2%20Crash%20I%20-%20Failure/03-Trondl-FraunhoferIWM-P.pdf).

[21]   G. R. Johnson, W. H. Cook, Fracture characteristics of three metals subjected to various strain, strain rates, temperature and pressures, Engineering Fracture Mechanics vol. 21, No.1, (1985) 31-48, http://dx.doi.org/10.1016/0013-7944(85)90052-9 (URL http://www.sciencedirect.com/science/article/pii/0013794485900529?via%3Dihub)

[22]   A. C. Bannister, S. J. Trail, The significance of the yield stress/tensile stress ratio to structural integrity, SINTAP Sub-Task 2.1 Report, 1996 (URL http://www.eurofitnet.org/sintap_BRITISH_STEEL_The_Significance_of_y-t_ratio.pdf)

[23]   A. C. Bannister, Yield stress/tensile stress ratio: Results of experimental programme SINTAP Sub-Task 2.3 Report, 1999 (URL http://www.eurofitnet.org/sintap_BRITISH_STEEL_BS-25.pdf)

[24]   A. C. Banister, J. Ruiz Ocejo, F. Gutierrez-Solana, Implications of the yield stress/tensile stress ratio to the SINTAP failure assessment diagrams for homogeneous materials, Engineering Fracture Mechanics vol. 67, (2000) 547-562, https://doi.org/10.1016/S0013-7944(00)00073-4 (URL http://www.sciencedirect.com/science/article/pii/S0013794400000734)

[25]   J. Healy, J. Billingham, Metallurgical considerations of the high yield to ultimate ratio in high strength steels for use in offshore engineering 14th International Conference OMAE1995, vol. 3: Materials Engineering, ASME (1995) 365 – 370.

[26]   R. L. Brockenbrough & Associates Inc., Effect of yield-tensile ratio on structural behaviour – High performance steels for bridge construction, Expanded Draft Final Report, ONR-AISI Agreement No. N00014-94-2-0002, 1995. (URL http://www.smdisteel.org/~/media/Files/SMDI/Construction/Bridges%20-%20HPS%20-%20Report%20%20Effect%20of%20Yield%20Tensile%20Ratio%20on%20Structural%20Behavior%20-%2006-06-1995.pdf).

[27]   J. Billingham, J. Healy, H. Bolt, High strength steels – The significance of yield ratio and work-hardening for structural performance, Marine Technology Directorate (MTD), Marine Research Review 9, (1997) 36 pages, ISBN 1-870553-27-6

[28]   BS EN 10025:6: +A1: 2009. Hot rolled products of structural steels – Part 6 Technical delivery conditions for flat products of high yield strength structural steels in the quenched and tempered condition, 2009

[29]   J. R. Davis, Tensile testing, 2nd Edition, ASM International, Materials Park, OH 44073-0002, ISBN: 0-87170-806-X, 2004.

[30]   M. S. Loveday, T. Gray, J. Aegerter, Tensile testing of metallic materials: A review EU Funded Project, TENSTAND-Work Package 1, final report with Contract Number G6RD-2000-00412, 2004.

[31]   ASTM E112, Standard test methods for determining average grain size, ASTM 2013, http://www.dx.doi.org/10.1520/E0112-13.